Nanonets

DOI: 10.1002/anie.200802788

Controllable Nanonet Assembly Utilizing a Pressure-Difference Method Based on Anodic Aluminum Oxide Templates**

Zhixun Luo, Yuanyuan Liu, Longtian Kang, Yaobing Wang, Hongbing Fu, Ying Ma, Jiannian Yao, and Boon H. Loo*

Self-assembly of organic molecules from solution is one of the simplest methods to generate ordered nanostructures with potentially new properties. In particular, nanostructured architectures on the macroscopic scale have possible applications in the fields of electronics, catalysis, and medicine.[1–7] However, controllable fabrication of nanostructured materials is still limited by the available processing methods. Template synthesis has been widely used as a controllable approach to achieve desirable nanostructured materials. Of the many different types of templates, anodic aluminum oxide (AAO)[8–14] offers clear advantages in the making of one-dimensional nanostructured materials and arrays; the AAO templates provide hexagonally packed, uniform pore arrays with a pore diameter that can be varied up to 200 nm. Amongst other applications, AAO has been used as a template for the syntheses of nanotubes for biomedicine and biotechnology,[10] $Bi_{1-x}Sb_x$ nanowires as thermoelectric wires,[11] SBA-15 nanorod arrays for protein separation and catalysis,[12] and lipid nanotube arrays as a model of cellular membranes.[14] Despite such progress, there have been few reports on the application of AAO as a substrate for the control of surface morphology on the macroscopic scale. Herein, we report for the first time the synthesis of the large-area (ca. 12 cm^2) nanonet architecture of 5,10,15,20-tetrakis(*p*-chlorophenyl)porphyrin (TClPP; $C_{44}H_{26}Cl_4N_4$) using the AAO template as a substrate. Figure 1 shows the 3D structure of the TClPP molecule and its stacking.

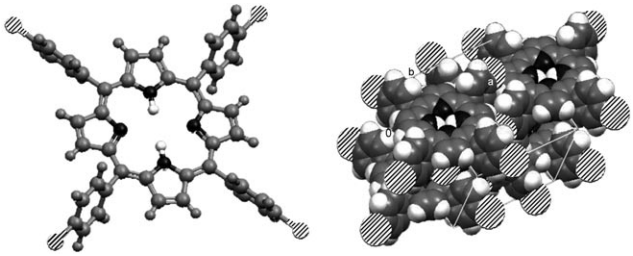

Figure 1. 3D structure of the TClPP molecule (left) and its stacking (right).

Alkylated polycyclic discotic molecules, such as porphyrins, are frequently employed as building blocks because of their ability to stack and form architectures and liquid-crystalline phases. We were able to use the stacking property of TClPP to successfully cultivate nanonet network architectures on the AAO templates. The TClPP nanonets were fabricated as follows. A 2-cm-diameter AAO disk about 15 μm in thickness was laid on a Buchner funnel fitted with a fritted disk. The funnel was then placed on a filter flask connected to a vacuum pump, which was used to maintain a pressure differential across the AAO disk. A solution of TClPP (1 mL, 0.13 M) in CH_2Cl_2 was added dropwise to the AAO template. TClPP nanonets of different meshes in accordance with the AAO pore sizes were thus grown on the rear of the AAO template, that is, the side opposite to that of TClPP deposition. This process was repeated several times to obtain nanoparticles of larger size. Experimental parameters, such as the pressure differential, concentration of the TClPP solution, and the number of times of solution deposition, affected the type and the quality of the nanostructures formed, which will be discussed below.

The morphology and size of the nanostructures were examined by field-emission scanning electron microscopy (SEM; Hitachi S-4300). Figures 2a and b show the SEM images of the TClPP nanonet structures formed on the AAO templates. It is evident that the nanonet structures were created as a result of uniform self-assembly of interlocking TClPP nanoparticles. The SEM images also suggest that the knots of the nanonets were formed by a single larger nanoparticle or by several assembled nanoparticles. In Figure 2a, the inner pores of the AAO substrate can be seen behind the floating nanonet. An advantage of this synthesis method was that the fabricated nanonet structure could be easily removed from the AAO substrate. Figure 2b shows the SEM image of a nanonet after it was removed from the substrate. The weblike nanonets showed ordered network structures with meshes mimicking the pore sizes of the AAO templates. Apparently the orderly pores of the AAO template aided the formation of the periodic pattern of the nanonets on the back surface of the template.

Three different pore sizes (50, 100, and 200 nm) of the AAO templates were tried in the making of nanonets. A small

[*] Dr. Z. Luo, Dr. Y. Liu, L. Kang, Y. Wang, Prof. H. Fu, Y. Ma, Prof. J. Yao
Beijing National Laboratory for Molecular Science
Institute of Chemistry
Chinese Academy of Sciences, Beijing 100190 (China)
Fax: (+86) 10-82616517
E-mail: jnyao@iccas.ac.cn
Prof. B. H. Loo
Department of Chemistry, Towson University (USA)

[**] We thank Prof. J. S. Ma (ICCAS) for providing the TClPP sample. This work was supported by the National Natural Science Foundation of China (Nos. 50221201, 90301010, 50502033, 50574083), the Chinese Academy of Sciences, the National Research Fund for Fundamental Key Project No. 973 (2006CB806200), and the National High-Tech R&D Program (863 Program) (2006AA03Z314).

Supporting information for this article is available on the WWW under http://dx.doi.org/10.1002/anie.200802788.

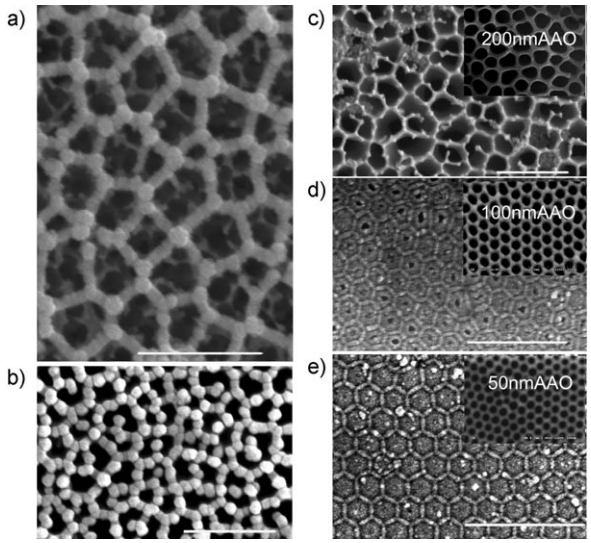

Figure 2. SEM images of TClPP nanonets cultivated on AAO templates with a pressure differential of 0.03 MPa. a) A floating nanonet; b) a freestanding nanonet after it was removed from the AAO template. c)–e) Patterns of the TClPP films in accordance with the shape of the AAO pores, with a pore size of c) 200, d) 100, and e) 50 nm. The insets show the neat AAO templates. Scale bars: 500 nm.

pressure differential was maintained across the deposited TClPP film during the fabrication process, which allowed nanonet structures of TClPP with a one-pore-one-mesh pattern to be formed on the rear of the AAO template. Although it was more difficult to fill the 200-nm pores of the template with the TClPP solution, thin meshes could still be obtained (Figure 2c). The AAO templates with smaller pore size (50 and 100 nm) were easily filled with the TClPP solution, and regular hexagon meshes of periodic patterns, which had the same distribution as the number of pores, were readily obtained (Figures 2d and e).

To understand the nature of the nanonet structures, X-ray diffraction (XRD) and absorption experiments were performed. Figure 3 shows the XRD pattern of the nanonet, together with those of powdered TClPP and single-crystalline TClPP from the crystal database. The XRD experiments were carried out on a Rigaku D/max-2500 rotating-anode X-ray diffractometer with graphite-monochromatized $Cu_{K\alpha}$ radiation (1.5418 Å). Unsurprisingly, the XRD pattern of the TClPP nanonet (measured in reflection mode) bears a closer resemblance to that of powdered TClPP than that of single-crystalline TClPP. However, compared to both these forms of TClPP, the TClPP nanonet exhibited only a few distinct diffraction peaks in the same region, which are assigned to the indices of the crystallographic planes of (001), (020), (121), and (410). The results suggest that the TClPP molecules assembled and grew along these crystallographic orientations to form the nanonet architecture.

In addition, absorption experiments performed on a Lambda 35 spectrometer reveal that the TClPP nanonet architecture exhibits different absorption behavior from that of TClPP in solution (see Figure 4). The TClPP in solution shows a strong monomer absorption at 418 nm, assigned to the Soret band, in addition to four barely visible peaks at 515,

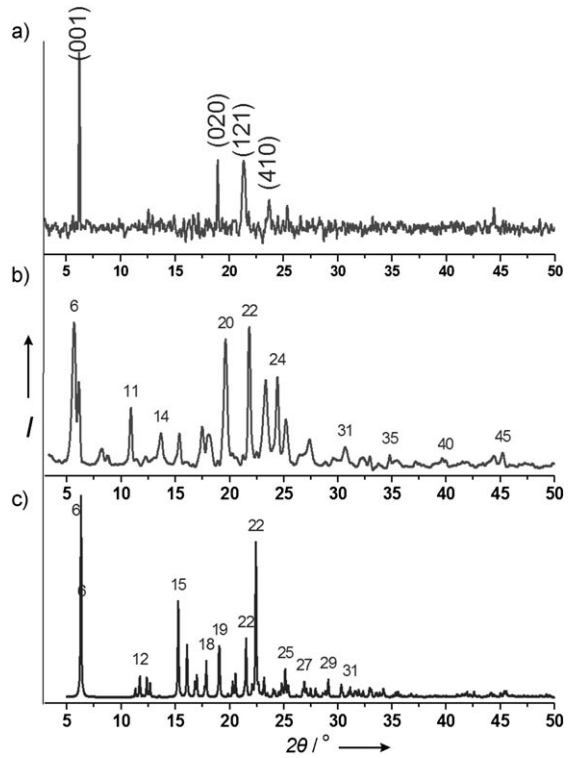

Figure 3. XRD patterns of a) TClPP nanonet, b) powdered TClPP, and c) single-crystalline TClPP.

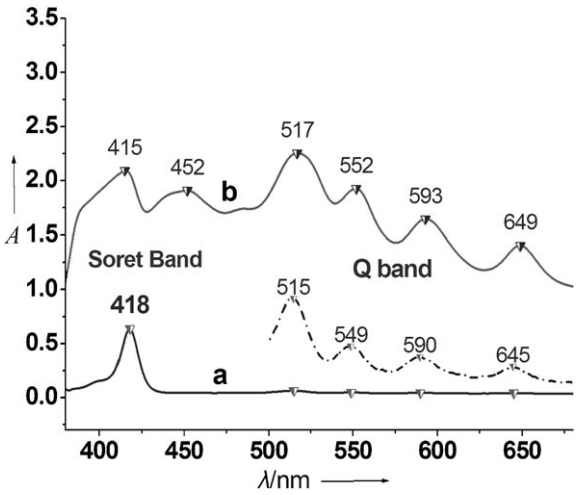

Figure 4. a) Absorption spectrum of 0.5×10^{-7} M TClPP in CH_2Cl_2 solution, which shows a strong Sorent band at 418 nm and four very weak peaks at 515, 549, 590, and 645 nm (referred to as the Q band and magnified immediately above). b) Absorption spectrum of the TClPP nanonet architecture, which resembles that of TClPP in solution (spectrum a) except for the presence of an additional peak at 452 nm.

549, 590, and 645 nm, assigned to the Q band (Figure 4a).[15,16] The TClPP nanonet, in contrast, shows a total of six peaks of strong intensity in the region (Figure 4b). Except for a small wavelength shift from the corresponding peak in solution, the 415 nm peak can be assigned to the Soret band. Likewise, the peaks at 517, 552, 593, and 649 nm are assigned to the Q band. The enhancement in the intensity of the Q band is attributed

to a lowering of molecular symmetry of TClPP in the nanonet architecture because of molecular aggregation.[17] The most interesting feature in the absorption spectrum of the TClPP nanonet architecture, however, is the appearance of the peak at 452 nm. This new peak can be attributed to J aggregation of the TClPP molecules in a head-to-tail arrangement.[18] Hence, the absorption results suggest the occurrence of J aggregates in the TClPP nanonets.

The XRD results show that the TClPP molecules assembled in quite an orderly manner and grew along some crystallographic orientations to form the nanonet architecture. According to the exciton theory of molecules,[19] different accumulations of molecules have different tilt angles to form a bulk assembly. The tilt angle refers to the angle between the line of centers of the molecules and the molecular long axis.[18] The angle value is greater than 54.7° for face-to-face (or side-by-side) accumulation, and is less than 54.7° for head-to-tail (or linear) accumulation. The approximate tilt angle for an accumulation of N molecules can be calculated according to Equation (1):

$$\Delta\nu = 2\frac{N-1}{N}\frac{<m^2>}{hr^3}(1-3\cos^2\alpha) \quad (1)$$

Herein, $\Delta\nu$ is the spectral shift from the monomer absorption, h is Planck's constant, r is the separation of centers, and α is the tilt angle between the line of centers and molecular long axes. The transition dipole moment of the monomer, $<m^2>$, equals $9.185\times10^{-39}\int_{\lambda_2}^{\lambda_1}\varepsilon(\mathrm{d}\lambda/\lambda)$; ε is the molar extinction coefficient in $\mathrm{mol\,L^{-1}\,cm^{-1}}$, λ is the wavelength, and λ_1 and λ_2 are the limits of a well-defined absorption band. Our calculated tilt angle was 54.4°, which is less than the critical angle of 54.7°. This result agrees with the conclusion of J aggregation from the absorption experiments.

It is remarkable that these nanoparticles assembled so uniformly on the rear of the AAO template. In fact, the nanonets extended all over the AAO substrate; a continuous nanonet network was found to cover the entire disk of surface area 12.6 $\mathrm{cm^2}$. This represents surface patterning of TClPP on a macroscopic scale (a representation of a portion of the nanonet network is given in Figure S2 in the Supporting Information). The result is significant in view of a recently reported finding on the construction of very large arrays of exceptionally long (up to 1 mm) lines by using porphyrin trimers, for possible uses in integrated circuits and microelectromechanical devices.[20]

As is known, self-assembly of molecules from solution often yields architectures that exhibit a high degree of order on the nanometer scale, but generates more disordered morphologies on the micrometer scale.[1] This is primarily a result of the nonuniform evaporation of solvent at surfaces.[1] Evaporation typically proceeds through dewetting of solution, which leads to the formation of holes in the liquid layer that eventually enlarge and coalesce until the solvent is completely evaporated. As we have found, an unordered film with some nonuniform rings was obtained when a drop of the TClPP solution was directly deposited on a flat silicon surface (Figure S4 in the Supporting Information). Hence, the perfect net morphology may be mainly due to the interfacial interaction between the TClPP molecules and the AAO template, known as the molecule–substrate effect.[1] However, no ordered nanonet architecture was obtained when the same AAO template was soaked in a TClPP solution (Figure S5 in the Supporting Information). Because TClPP is a large macrocyclic molecule, the question arises whether the size of the molecule is the main factor in the stability of the nanonet architecture. This possibility can be ruled out, as we have found that nanonet architectures could also be obtained from smaller organic molecules, such as perylene (Figure S9 in the Supporting Information).

We now look at the parameters, namely, the pressure differential across the deposited films, the concentration of the TClPP solution, and the number of times of solution deposition, which might affect the formation of the nanonet assembly. Figures 5a and b show SEM images of the films formed on the AAO templates at pressure differentials of

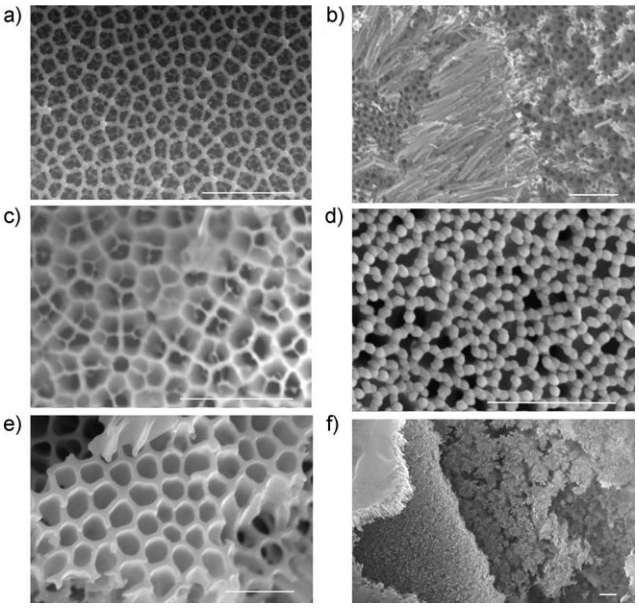

Figure 5. SEM images of TClPP nanostructures cultivated on AAO templates (100-nm pores) at a pressure differential of a) 0.04 or b) 0.07 MPa; at a TClPP concentration of c) 1.0×10^{-5} or d) 0.13 M (both at 0.04 MPa, deposition 20 times); with the number of depositions e) 30 or f) 50 times (at a pressure differential of 0.03 MPa). Scale bars: 1 μm.

0.04 MPa (or 300 Torr) and 0.07 MPa (or 525 Torr), respectively. The experimental results show that the optimal pressure differential for obtaining nanonets was about 0.03–0.04 MPa. In this case, a very regular, ordered nanonet was formed on the AAO substrate (Figure 5a). However, when the applied pressure differential was higher than the optimal value, no nanonet structures were obtained; nanofibers were formed instead (Figure 5b). On the other hand, if not enough pressure differential was maintained, an ultrathin film was formed on the surface. It is believed that the pressure differential caused the TClPP molecules to migrate through

the AAO pores and form bubbles. Dewetting occurred when the bubbles broke and the molecules assembled into nanoring arrangements on the pore edge to form periodic patterns. This interaction could also be directional and bubbles would merge into each other.[1] With the evaporation of the solvent, the solute molecules would then form nanonet architectures. It was noted in our experiments that the pressure difference was an essential factor in obtaining nanonet architectures.

Figures 5c and d indicate that different nanostructures were obtained with different TClPP solution concentrations. When the concentration was low (1×10^{-5} M), the solution went directly through the pores with little self-assembly behavior. As a result, a thinner nanonet architure was obtained (Figure 5c). When a near-saturated solution (0.13 M) was used, there was a greater tendency of the nanoparticles to assemble into a nanonet architecture. Hence, larger TClPP nanoparticles were formed and the nanonets were produced out of these larger nanoparticles (Figure 5d).

The concentration dependence, substrate effect, and pressure parameter indicated that a balance of equilibrium between the self-assembly, dynamic migration, and dewetting processes must be achieved[20] for the making of large-scale nanonets. In addition, when the molecules assemble and interact with one another through weak van der Waals forces, the number of depositions is a desirable criterion to control the nanonet architecture (Figures 5e and f). Figure 5e shows a honeycomb-like nanostructure with 30 depositions of TClPP solution, whereas Figure 5f shows a multilayer architecture with 50 depositions.

The formation of a nanonet assembly was mainly controlled by the substrate effect and the dynamic control process. In other words, it was affected by the pinhole migration of the liquid phase along the AAO pores because of the nature of the substrate used. Indeed, it was observed that some tubular structures were formed in the pores. The TClPP solution migrated through the AAO pores to form bubbles and then assembled into the mesh patterns of the nanonet architectures, thus giving rise to the pinhole mechanism which is actually a well-known "edge effect" phenomenon.[17] Bubble formation at the rear of the AAO substrate as a result of a pressure differential, and the radial flow of molecules at the pores edges, together with their tendency to self-assemble brought forth periodic patterns of nanorings when the bubbles broke. However, the bubbles may further migrate and also adjoin each other to form a network of nanonet architecture with one-hole-one-mesh or one-hole-multiple-mesh patterns. The topographical features of the AAO templates rendered them ideal hosts for the formation of regular and uniform nanonet assemblies of TClPP.

In summary, a large network (ca. 12 cm^2) of TClPP with a nanonet architecture has been fabricated on AAO templates by applying a pressure differential across the deposited TClPP films on the templates. Stable nanonets can be reproduced with the same mesh patterns as the hexagonally packed, uniform pore arrays of the AAO templates. While the extension of the present findings to other molecules or systems remains to be explored, the unique structural features of the nanonets may find applications in molecular filtering as well as in catalysis.

Received: June 13, 2008
Published online: October 10, 2008

Keywords: aggregation · nanostructures · porphyrinoids · self-assembly · template synthesis

[1] V. Palermo, P. Samori, *Angew. Chem.* **2007**, *119*, 4510; *Angew. Chem. Int. Ed.* **2007**, *46*, 4428.
[2] a) H. B. Fu, J. N. Yao, *J. Am. Chem. Soc.* **2001**, *123*, 1434; b) L. T. Kang, Z. C. Wang, Z. W. Cao, Y. Ma, H. B. Fu, J. N. Yao, *J. Am. Chem. Soc.* **2007**, *129*, 7305.
[3] F. Bertorelle, F. Rodrigues, S. Fery-Forgues, *Langmuir* **2006**, *22*, 8523.
[4] J. S. Hu, Y. G. Guo, H. P. Liang, L. J. Wan, L. Jiang, *J. Am. Chem. Soc.* **2005**, *127*, 17090.
[5] K. Balakrishnan, A. Datar, T. Naddo, J. Huang, R. Oitker, M. Yen, J. Zhao, L. Zang, *J. Am. Chem. Soc.* **2006**, *128*, 7390.
[6] Y. Kaneko, S. Shimada, T. Fukuda, T. Kimura, H. Yokoi, H. Matsuda, H. Onodera, H. Kasai, S. Okada, H. Oikawa, H. Nakanishi, *Adv. Mater.* **2005**, *17*, 160.
[7] S. Kim, Q. D. Zheng, G. S. He, D. J. Bharali, H. E. Pudavar, A. Baev, P. N. Prasad, *Adv. Funct. Mater.* **2006**, *16*, 2317.
[8] H. Masuda, K. Fukuda, *Science* **1995**, *268*, 1466.
[9] Y. Cui, C. M. Lieber, *Science* **2001**, *291*, 851.
[10] R. Gasparac, P. Kohli, M. O. Mota, L. Trofin, C. R. Martin, *Nano Lett.* **2004**, *4*, 513.
[11] A. L. Prieto, M. M. Gonzalez, J. Keyani, R. Gronsky, T. Sands, A. M. Stacy, *J. Am. Chem. Soc.* **2003**, *125*, 2388.
[12] Q. Y. Lu, F. Gao, S. Komarneni, T. E. Mallouk, *J. Am. Chem. Soc.* **2004**, *126*, 8650.
[13] S. Chia, J. Urano, F. Tamanoi, B. Dunn, J. I. Zink, *J. Am. Chem. Soc.* **2000**, *122*, 6488.
[14] A. I. Smirnov, O. G. Poluektov, *J. Am. Chem. Soc.* **2003**, *125*, 8434.
[15] E. S. Emerson, M. A. Conlin, A. E. Rosenoff, K. S. Norland, H. Rodriguez, D. Chin, G. R. Bird, *J. Phys. Chem.* **1967**, *71*, 2396.
[16] J. P. Macquet, M. M. Millard, T. Theophanide, *J. Am. Chem. Soc.* **1978**, *100*, 4741.
[17] R. D. Deegan, O. Bakajin, T. F. Dupont, G. Huber, S. R. Nagel, T. A. Witten, *Nature* **1997**, *389*, 827.
[18] Z. Luo, A. Peng, H. Fu, Y. Ma, J. Yao, B. H. Loo, *J. Mater. Chem.* **2008**, *18*, 133–138.
[19] M. Kasha, H. R. Rawls, M. A. El-Bayoumi, *Pure Appl. Chem.* **1965**, *11*, 371.
[20] R. V. Hameren, P. Schon, A. M. Buul, J. S. Hoogboom, V. Lazarenko, J. W. Gerritsen, H. Engelkamp, P. C. M. Christianen, H. A. Heus, J. C. Maan, T. Rasing, S. Speller, A. E. Rowan, J. A. A. W. Elemans, R. J. M. Nolte, *Science* **2006**, *314*, 1433.

